CVD Growth of N-Doped Carbon Nanotubes on Silicon Substrates and Its Mechanism

Maoshuai He,[†] Shuang Zhou,[†] Jin Zhang,*[,†] Zhongfan Liu,*[,†] and Colin Robinson[‡]

Key Laboratory for the Physics and Chemistry of Nanodevices, Center for Nanoscale Science and Technology (CNST), College of Chemistry & Molecular Engineering, Peking University, Beijing 100871, People's Republic of China, and Division of Oral Biology, University of LEEDS, Clarendon Way, Leeds LS2 9LU, UK

Received: November 9, 2004; In Final Form: March 16, 2005

In the present study, we report the chemical vapor deposition (CVD) of nitrogen-doped (N-doped) aligned carbon nanotubes on a silicon (Si) substrate using ferrocene ($Fe(C_5H_5)_2$) as catalyst and acetonitrile (CH_3CN) as the carbon source. The effect of experimental conditions such as temperature, gaseous environment, and substrates on the structure and morphology of N-doped carbon nanotubes arrays is reported. From XPS and EELS data, it was found that the nitrogen content of the nanotubes could be determined over a wide range, from 1.9% to 12%, by adding the addition of hydrogen (H_2) to the reaction system. It was also shown by SEM that N-doped carbon nanotube arrays could be produced on Si and SiO_2 substrates at suitable temperatures, although at different growth rates. Using these concentrations, it was possible to produce three-dimensional (3D) carbon nanotubes architectures on predetermined Si/SiO_2 patterns. The mechanism underlying the effect of nitrogen containing carbon sources on nanotube formation was explored using X-ray photoelectron spectroscopy (XPS).

Introduction

Since their discovery,[1] carbon nanotubes have been the subject of considerable attention because of their remarkable electronic and mechanical properties.[2−4] Their peculiar electronic properties, especially in field-emission, facilitate a wide range of applications including scanning probe sensors, cold cathode flat panel displays, as well as vacuum microelectronics.[5−7] Most research on nanotubular carbon structures has focused on pure carbon nanotubes. The electronic response of pure carbon nanotubes approaches that of metallic or semiconducting materials and depends on helicity, morphology, number of layers, tube diameter, and defects.[8−10] However, up to now, it has not been possible to precisely control any of these parameters during the growth process. This makes the electronic performance of pure carbon nanotubes highly unpredictable.

An effective method of controlling electronic properties of carbon nanotubes is described by introducing nitrogen (N) during the growth process. The additional electrons contributed by the nitrogen atoms provide electron carriers for the conduction band;[11] N-doped nanotubes were found to be either metallic or narrow energy gap semiconductors,[12,13] thus offering the possibility of greater electrical conductivity as compared to pure carbon nanotubes. Clearly CN_x nanotubes of controlled composition would prove extremely advantageous in the fabrication of materials with tailored electronic and mechanical properties.

On this basis, a theoretical consideration of possible models for C_3N_4 and CN tubules has been proposed.[14] Several research groups have reported the synthesis of well-aligned N-doped carbon nanotubes using the CVD approach. Most of the syntheses relied on catalytic pyrolysis of a range C/N sources.[15−20] Terrones and co-workers generated well-aligned N-doped carbon nanotubes by pyrolyzing triazine, melamine, and C_{60} in an ammonia atmosphere.[15−17] The Rao group produced a high yield of well-aligned CN_x nanotubes by carrying out pyrolysis of pyridine over iron or cobalt nanoparticle catalysts.[18,19] A further approach was to use aerosol-assisted decomposition of dimethylformamide in the presence of Fe_2O_3 and MoO_3 composite catalyst, which produced highly nitrogen-doped (∼20 at. %) multiwalled carbon nanotubes. These multiwalled carbon nanotubes exhibited excellent field emission performance.[20]

From these data, it is clear that controlling the concentration of nitrogen atoms in carbon nanotubes is an excellent means of modulating the electrical properties of the final carbon nanotubes. Despite this, good strategies for controlled N doping are still not available.

For many applications, Si, SiO_2, glass, and quartz substrates have been used as substrates for carbon nanotube growth. Most applications, however, require a fabrication method capable of producing aligned carbon nanotubes with uniform morphologies and periodic structures to meet specific device requirements.

As a result of this, considerable progress has been made in the fabrication of 2D carbon nanotube architectures on different substrates and using different catalysts.[21,22] Wei et al. demonstrated organized, well-aligned nanotube growth on preselected SiO_2 sites, normal to a Si/SiO_2 patterned template. No carbon nanotube growth occurred on the Si domains of the template.[22] The mechanism by which nanotubes form on the SiO_2 but not Si is still obscure. Jung et al., however, investigated the reason for lack of growth on Si substrate by several high-resolution techniques (HRTEM, selective area electron beam diffraction, etc.).[23] They demonstrated that catalytically inactive iron silicide ($FeSi_2$)/iron silicate ($FeSiO_4$) particles formed on the Si substrate during high-temperature processing.

As compared to 2D carbon nanotube structures, 3D structures have an even greater range of potential applications, for example, in photonic devices, data storage, and as ultra-hydrophobic

* Corresponding authors. Tel./Fax: 00-86-10-6275-7157. E-mail: jinzhang@pku.edu.cn (J.Z.), lzf@chem.pku.edu.cn (Z.L.).
[†] Peking University.
[‡] University of LEEDS.

10.1021/jp044868d CCC: $30.25 © 2005 American Chemical Society
Published on Web 04/15/2005

materials. Quartz substrates, which had been patterned with aluminum film, have been used to fabricate 3D aligned carbon nanotube by pyrolysis of FePc.[24] Huang et al. also described a method for controlled fabrication of 3D carbon nanotube architecture on glass by stamp printing bimetallic Fe−Pt/polymer catalyst onto the substrate.[25] Using a multistep processes, he also produced large patterned areas of 3D aligned carbon nanotubes based on the pyrolysis of FePc.[26] Despite this activity, there is still little definitive information on the role of substrate and catalyst in nanotube formation.

In the work reported here, controllable synthesis of large areas of aligned CN_x nanotubes by pyrolyzing $CH_3CN/Fe(C_5H_5)_2$ both on SiO_2 and Si substrates has been achieved over the temperature range 750−900 °C. As temperatures were increased, the specific diameters of carbon nanotubes decreased on Si substrates as compared to a well-documented increase with temperature on SiO_2. The reasons for this are most likely due to different formation mechanisms of catalyst particles during the growth process. Most attention has been paid to nanotubes grown on Si substrates, because of the rather rapid growth rate and good alignment obtained. The presence of N in the carbon nanotubes (from CH_3CN) was demonstrated using X-ray photoelectron spectroscopy (XPS) and electron energy-loss spectroscopy (EELS) confirmed. More importantly, control of N content over the range from 1.9% to 12.2% was achieved by adding H_2 to the system during growth. By the use of photolithography to produce patterned substrates, it proved easy to effectively fabricate large areas 3D aligned carbon nanotube patterns. Using XPS, we have proposed possible reasons for the different behaviors of pure carbon sources as compared to CH_3CN on Si substrates. Such data will lead to a better understanding of growth mechanisms for 3D carbon nanotubes.

Experimental Section

A. Growth of Carbon Nanotubes. The substrates used were SiO_2 (SiO_2 thickness $t_{ox} = 100$ nm) or Si(111) wafers. Before use, Si and SiO_2 wafers were cleaned with acetone, ethanol, deionized water, and piranha solution (H_2O_2:H_2SO_4 = 3:7). Patterning of Si/SiO_2 substrates was effected by photolithography followed by wet etching. The CVD growth system was similar to that of Terrones et al.,[16] which depended on a two-stage furnace fitted with high-resolution temperature controllers. A solution of 0.02 g/mL $Fe(C_5H_5)_2$ in CH_3CN was prepared. In the preheating furnace, the temperature was raised to and maintained at 230 °C with flow of nitrogen gas (N_2) at 500 standard cubic centimeters per minute (sccm). When the temperature in the reaction zone reached 850 °C, the solution was fed continuously into the quartz reactor through a syringe pump at a feed rate of 8.00 mL/h for all runs. The reaction was usually maintained for 15 min; that is, a total of 2.00 mL of solution would be injected into the CVD system. The system was allowed to cool to room temperature while maintaining nitrogen flow.

B. Characterization of Carbon Nanotube Arrays. To characterize the structure and the composition of the carbon nanotubes obtained, scanning electron microscopy (SEM, XL30S-FEG, 15 kV), transmission electron microscopy (TEM, JEM200CX, 120 kV), EELS attached to a HRTEM (FEI Tecnai F30 FEG, 300 kV), and Raman spectroscopy (Renishaw micro-Raman 1000, 632.8 nm) were employed. XPS analysis was performed with an Axis Ultra spectrometer (Kratos, UK), using Mono Al K_α (1486.71 eV) radiation at a power of 225 W (15 mA, 15 kV). To compensate for surface charge effects, binding energies were calibrated using the C1s hydrocarbon peak at 284.8 eV.

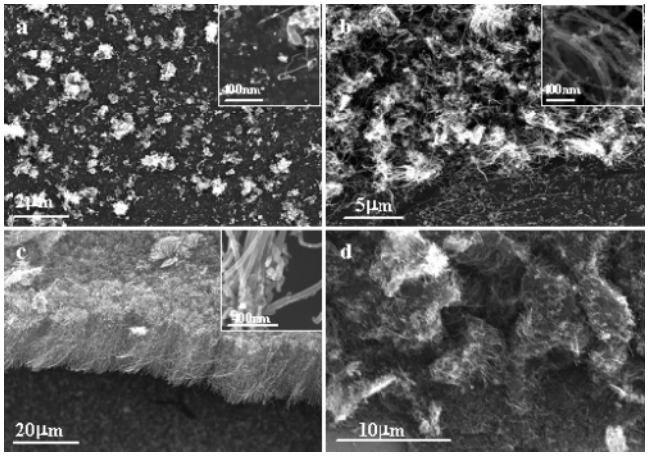

Figure 1. SEM micrographs of carbon nanotubes grown on SiO_2 substrate at (a) 750 °C, (b) 800 °C, (c) 850 °C, and (d) 900 °C; insets are magnified SEM images.

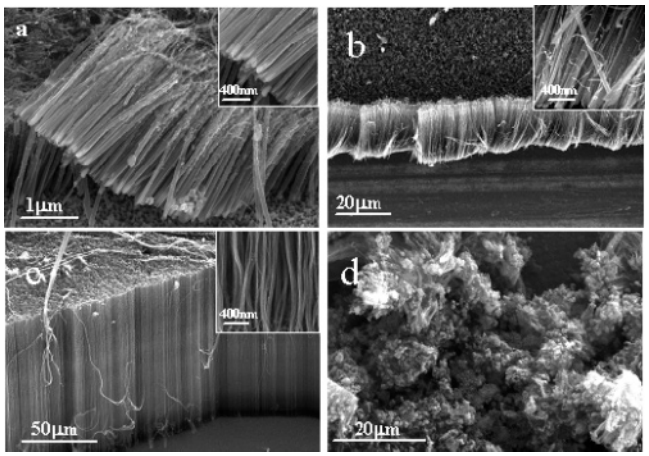

Figure 2. SEM micrographs of carbon nanotubes grown on Si substrate at (a) 750 °C, (b) 800 °C, (c) 850 °C, and (d) 900 °C; insets are magnified SEM images.

Results and Discussion

A. The Effect of Temperature on the Growth of Carbon Nanotube Arrays. In most cases, $Fe(C_5H_5)_2$ decomposed and formed small iron nanoparticles that acted as a catalyst for carbon nanotube formation.[22] Temperature had a great effect on the morphology and alignment of the carbon nanotubes. In our system, at temperature ranging from 750 to 900 °C, carbon nanotubes were formed both on SiO_2 and on Si substrates.

Figure 1 depicts SEM images for nanotubes grown on SiO_2 with identical ferrocene concentrations but at different temperatures. It can be seen that only at 850 °C could well-aligned carbon nanotubes with lengths reaching up to 20 μm be formed (Figure 1c). From insets of Figure 1a−c, which are magnified images of the nanotubes, we can see that diameter tended to increase with temperature, although there was a broad distribution of diameters.

Because of the unsuitable interaction between iron nanoparticles and Si substrate (formation of FeSi or $FeSiO_4$), it was once considered to be almost impossible to synthesize carbon nanotubes on Si substrates using ferrocene as a catalyst.[22,23] However, using instead CH_3CN as the carbon source, it did prove possible to grow aligned carbon nanotubes on Si over a relatively wide temperature range (Figure 2). At 750 °C (Figure 2a), aligned short (~2 μm) carbon nanotubes were obtained. At 800 °C (Figure 2b), well-aligned carbon nanotubes were obtained with average lengths of about 18 μm. At 850 °C, the

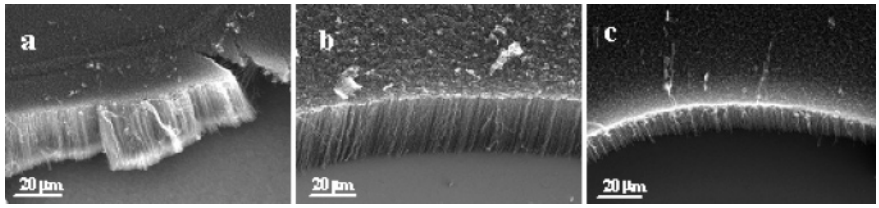

Figure 3. (a) SEM micrographs of aligned CNTs grown at 850 °C with a flow rate of H_2 = 100 sccm, (b) 300 sccm, and (c) 600 sccm.

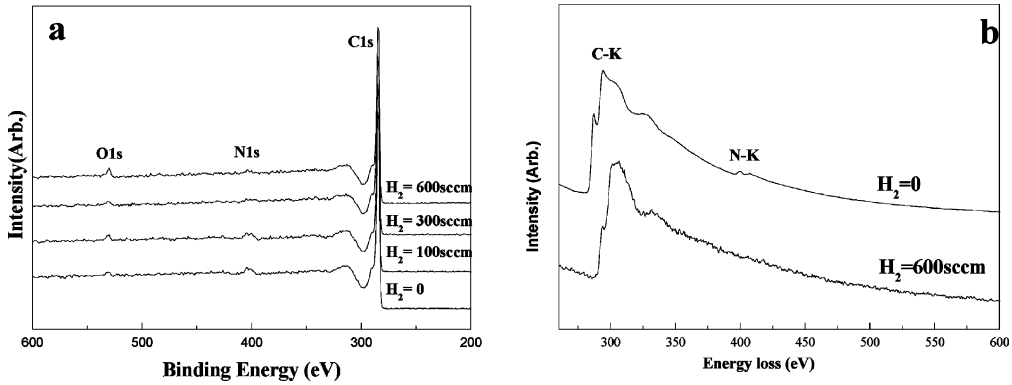

Figure 4. (a) XPS spectra of the N-doped carbon nanotubes grown at 850 °C with a flow rate of H_2 = 0, 100, 300, and 600 sccm. (b) EELS data for the N-doped carbon nanotubes grown at 850 °C without H_2 and with H_2 = 600 sccm.

length of the tubes increased to more than 90 μm (Figure 2c). At 900 °C, nanotube alignment was lost and only a small number of nanotubes were formed, with amorphous carbonaceous deposits on tube surfaces (Figure 2d).

Tube diameter was also determined by temperature. As shown in the insets of Figure 2a−c, tube diameter decreased with the temperature increase. At 750 °C, the diameter of the tubes was about 50 nm, while at 850 °C tube diameters were reduced to about 20 nm. This is contrary to results reported by other workers especially using SiO_2 as substrate,[27] in which tube diameter usually increased with the elevation of temperature. This may indicate that the formation mechanism of catalyst particles is quite different when Si is used as substrate.

B. Controlled Growth of Carbon Nanotube Arrays with Different Nitrogen Content. The gaseous environment has been shown to be a key parameter that influences CVD growth. NH_3, for example, has been added to reaction systems to produced N-doped carbon nanotubes.[18,28] In our current studies, we have also introduced H_2 to fine-tune the N contain of carbon nanotubes. During the growth process, 100, 300, or 600 sccm H_2 was put through the reaction system accompanied by the same feeding rate of the mixture solution. Figure 3a−c shows SEM micrographs of carbon nanotubes grown on Si substrates at 850 °C with 100, 300, and 600 sccm H_2, respectively. These images indicate the tubes were still aligned well; the apparent difference in their lengths is due to the variation of tilt angle at SEM imaging. N content was demonstrated by XPS analysis (Figure 4a). All spectra show the C1s, N1s, and O1s signals, corresponding to the main peaks centered at 284.8, 401.1, and 531.4 eV, respectively. The strong C peak that is assigned to a π^* feature associated with sp^2-hybridized carbon indicates that the major component is carbon. The O peak mainly arises from the oxygen absorbed on the surface of carbon nanotubes and the substrate on which carbon nanotubes were grown. Surface defects would also contribute to the O peak. The ratio of carbon to nitrogen was estimated from the ratio of the integrated areas beneath the C1s and N1s signal. It can be clearly seen that the N content in the tubes decreased gradually with increasing H_2 flow rate. At a flow rate of 600 sccm, the N content in the nanotubes was reduced to ~1.90%.

To get a more precise value for N content, EELs attached to a HRTEM was used. Figure 4b (the upper one) corresponds to a typical EELs spectrum of CNTs grown without H_2, which exhibited the characteristic K-shell ionization edges for C and N at ~286.3 and ~400.0 eV, respectively. The sharp 286.3 eV peak is due to transitions from the 1s core level to the π^* band, and the band starting at 293.7 eV is assigned to transitions to the p-orbits merging with part of the broad σ^* band.[29,30] The carbon K-edge spectrum revealed the characteristic σ^* feature, from the sp^2 hybridization of carbon.[31] Likewise, the well-defined π^* adsorption feature for the N K-edge corresponds to the sp^2 bonding of N in hexagonal nitrogen/carbon conformation. From the quantification of the two edges, it was estimated that N content in the nanotubes was about 12%. However, for nanotubes grown with 600 sccm H_2, there was no N characteristic K-shell ionization edge, which suggests that the N content was too low to detect (the lower one in Figure 4b).

The mechanism by which H controls N content can be interpreted as indicated in ref 32. At high temperatures, CN• and CH_3• free radicals are produced as active fragments during the formation of N-doped carbon nanotubes. During the reaction, added H_2 is likely to generate HCN: $H_2 + CN\bullet = HCN + H\bullet$, because HCN is more stable and less reactive than CH_3CN in the gas phase. HCN would diffuse out of the reaction zone, thus restricting the availability of N for doping into the nanotubes.

C. Fabrication of 3D N-Doped Carbon Nanotubes Procedure and Architecture of Product. The finalized procedure for producing 3D carbon nanotubes is outlined in Figure 5. The SiO_2 substrate layer (t_{ox} = 100 nm) was prepared and patterned by conventional photolithography. Subsequent etching was performed using hydrofluoric acid. 3D carbon nanotubes were then produced by pyrolysis of CH_3CN and $Fe(C_5H_5)_2$ solution at 850 °C for 15 min with a feeding rate of 8.00 mL/h. Figure 6a is a typical SEM image of a large area of carbon nanotubes. At higher magnification (Figure 6b), carbon nanotubes can be seen as straight and densely packed. This arrangement was affected by the patterned substrate. At small pattern sizes, aligned or flowerlike carbon nanotube architectures could be formed (Figure 6c,d). In terms of length, under the same

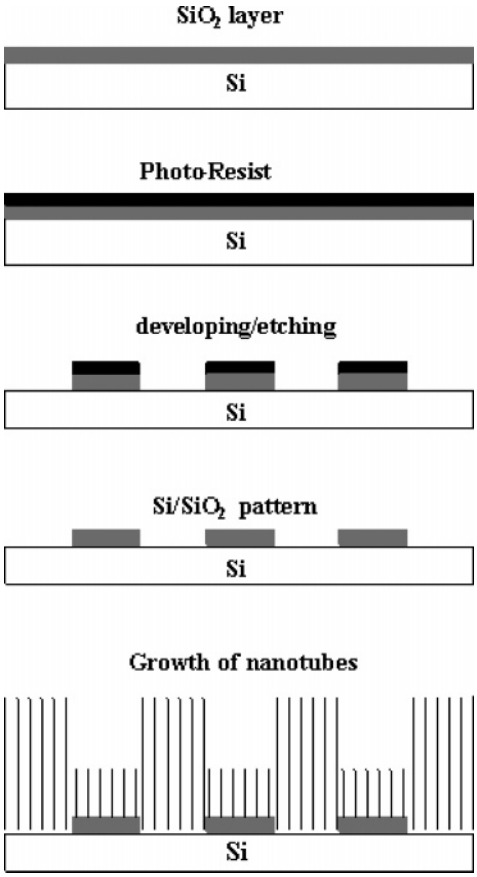

Figure 5. Schematic illustration of the procedure for the growth of three-dimensional carbon nanotube architectures.

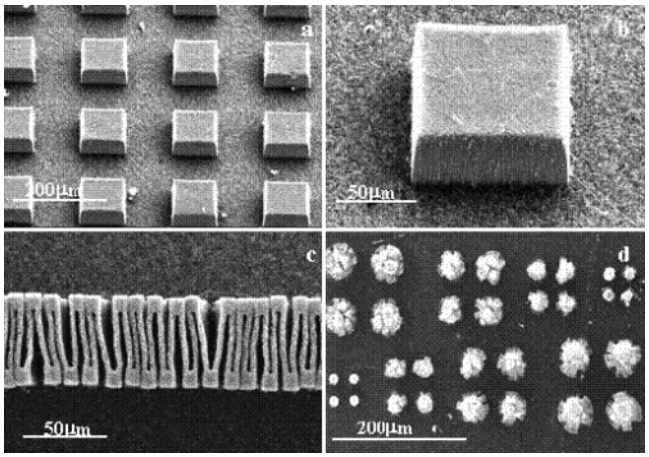

Figure 6. Typical SEM micrographs of 3D architectures resulting from different shapes and sizes of Si patterns: (a) square arrays and (b) magnified image of (a). (c) The Great Wall-like arrays and (d) flowerlike arrays. The backgrouds are all short well-aligned carbon nanotubes grown on SiO_2.

conditions of reaction time and temperature, carbon nanotubes grown on Si were much longer than those grown on SiO_2.

D. Growth Mechanism of N-Doped Carbon Nanotubes on Si Substrate: Effect of Carbon Source. In an effort to elucidate the growth mechanism of N-doped carbon nanotubes on Si substrate, XPS was used to characterize the substrates after the growth process. Three sample types were investigated: (I) SiO_2 substrate after growth of carbon nanotubes using hexane as carbon resource; (II) Si substrate after growth of nanotubes using hexane as carbon source; and (III) Si substrate after growth using acetonitrile as carbon source. $Fe(C_5H_5)_2$ was

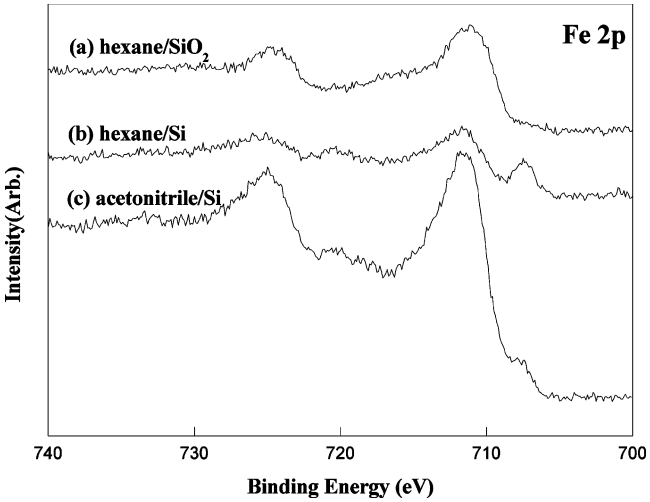

Figure 7. XPS spectra of the Fe 2p region on the substrate after scratching away the nanotubes (a) using hexane as carbon resource and SiO_2 as substrate and (b) using Si as substrate. (c) Using acetonitrile as carbon resource and Si as substrate.

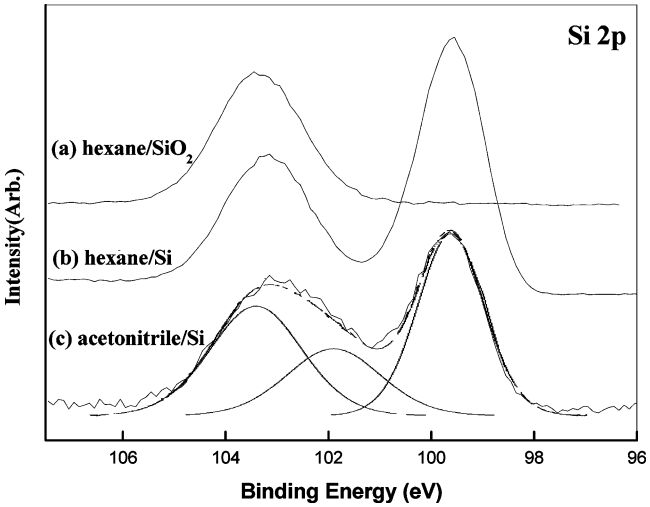

Figure 8. XPS spectra of the Si 2p region on the substrate after scraping off carbon nanotubes (a) using hexane as carbon resource and SiO_2 as substrate, (b) using hexane as carbon resource and Si as substrate, and (c) using CH_3CN as carbon resource and Si as substrate.

used as catalyst for all cases. Prior to XPS analysis, the tubes have been scratched away from the substrates (there were no tubes grown on II), and the samples were then transferred into the analysis chamber at room temperature.

The Fe2p and Si2p core lines of sample I acquired at room temperature are shown in Figures 7a and 8a, respectively. The Si2p peak, shown in Figure 8a, shows only a main component at 103.3 eV, corresponding to silicon dioxide. No other forms of silicon were detected. On the other hand, the position of the Fe $2p_{3/2}$ line (711.1 eV) in Figure 7a revealed that almost all of the Fe had been oxidized, because of the high reactivity of iron nanoparticles. No other form of Fe was detected on the substrate. This indicated that iron nanoparticles, formed by decomposition of $Fe(C_5H_5)_2$, did not react with the SiO_2 substrate and acted as the catalyst for carbon nanotube growth.

As for sample II, the Si2p doublet, shown in Figure 8b, shows a component at 99.3 eV corresponding to pure Si and an oxide component. The oxide peak is probably due to the existence of a native SiO_2 layer. The position of the Fe $2p_{3/2}$ line, centered at 711.1 eV, is similar to that of sample I (Figure 7b). However, the appearance of a strong Fe $2p_{3/2}$ on the low binding energy

side of the main line points to the presence of an iron silicide.[33] This is in agreement with the previous reports.[23] In fact, the formation of iron silicide is most likely the main reason for lack of growth of pure carbon nanotubes on Si substrates. However, the peak centered at around 707.3 eV was strongly reduced in sample III (Figure 7c), probably due to the recovery of iron particles.

When CH_3CN arrives in the reaction zone, the species CN•, as opposed to C fragment from a pure carbon source, is thought to react with $FeSi_2$, thus reactivating the iron for the growth of N-doped carbon nanotubes. This is almost certainly the reason for the existence of the relatively small $FeSi_2$ peak. The Si2p of III also confirms this conjecture, Figure 8c, because the oxide peak is much wider than that of Figure 8b. Using a fitting procedure, this peak can be divided into two: one would be silicon oxide, centered at 103.3 eV; the other peak shifted to a lower binding energy (101.8 eV), corresponds to silicon nitride[34] (the fwhm is similar to that of silicon oxide), which may derive from the reaction between $FeSi_2$ and CN• species. In summary, the existence of N-containing fragments is the paramount factor for the growth of carbon nanotubes on Si substrates. In fact, using CH_3CN as a carbon resource, N-doped carbon nanotubes can be grown on some unconventional substrates, such as Au and Cu substrates (results not shown); this is also due to the reactivation of iron catalyst particles by N-containing fragments. The in-situ growth of carbon nanotubes on more substrates widens their potential applications in nanotechnology.

Summary

In summary, the main results presented in the Article are as follows. (1) Using $Fe(C_5H_5)_2$ as catalyst and CH_3CN as carbon source, aligned N-doped carbon nanotubes have been successfully grown on Si substrates. (2) The N content could be effectively modulated over a wide range simply by adding H_2 to the reacting system. (3) Combined with photolithography, we also present a simple and feasible method for the fabrication of various 3D architectures. (4) Based on XPS data, a mechanism for the growth of N-doped carbon nanotubes on Si substrates has been proposed.

Acknowledgment. This work was supported by the National Natural Science Foundation of China (NSFC 90206023), the Ministry of Science and Technology of China (2001CB6105), and the FOKYING TUNG Education Foundation (94012).

References and Notes

(1) Iijima, S. *Nature* **1991**, *354*, 56.
(2) Yakobson, B. I.; Brabec, C. J.; Bernholc, J. *Phys. Rev. Lett.* **1996**, *76*, 2511.
(3) Wong, E. W.; Sheehan, P. E.; Lieber, C. M. *Science* **1997**, *277*, 1971.
(4) Falvo, M. R.; Taylor, R. C.; Helser, A.; Chi, V.; Brooks, F. P.; Washburn, S.; Superfine, R. *Nature* **1999**, *397*, 236.
(5) Fan, S.; Chapline, M. G.; Franklin, N. R.; Tombler, T. W.; Cassell, A. M.; Dai, H. *Science* **1999**, *283*, 512.
(6) Ren, Z. F.; Huang, Z. P.; Xu, J. W.; Wang, J. H.; Bush, P.; Siegal, M. P.; Provencio, P. N. *Science* **1998**, *282*, 1105.
(7) Li, W. Z.; Xie, S. S.; Qian, L. X.; Chang, B. H.; Zou, B. S.; Zhou, W. Y.; Zhao, R. A.; Wang, G. *Science* **1996**, *274*, 1701.
(8) Hamada, N.; Sawada, S.; Oshiyama, A. *Phys. Rev. Lett.* **1992**, *68*, 1579.
(9) Saito, R.; Fujita, M.; Dresselhaus, G.; Dresselhaus, M. S. *Appl. Phys. Lett.* **1992**, *60*, 2204.
(10) Odom, T. W.; Huang, J.-L.; Kim, P.; Lieber, C. M. *J. Phys. Chem. B* **2000**, *104*, 2794.
(11) Terrones, M.; Ajayan, P. M.; Banhart, F.; Blase, X.; Carroll, D. L.; Charlier, J. C.; Crzerw, R.; Foley, B.; Grobert, N.; Kamalakaran, R.; Kohler-Redlich, P.; Rühle, M.; Seeger, T.; Terrones, H. *Appl. Phys. A* **2002**, *74*, 355.
(12) Miyamoto, Y.; Cohen, M. L.; Louie, S. G. *Solid State Commun.* **1997**, *102*, 605.
(13) Huang, Y.; Gao, J.; Liu, R. *Synth. Met.* **2000**, *113*, 251.
(14) Liu, A. Y.; Cohen, M. L. *Science* **1989**, *245*, 841.
(15) Terrones, M.; Grobert, N.; Olivares, J.; Zhang, J. P.; Terrones, H.; Kordatos, K.; Hsu, W. K.; Hare, J. P.; Townsend, P. D.; Prassides, K.; Cheetham, A. K.; Kroto, H. W.; Walton, D. R. M. *Nature* **1997**, *388*, 52.
(16) Terrones, M.; Redlich, P.; Grobert, N.; Trasobares, S.; Hsu, W. K.; Terrones, H.; Zhu, Y. Q.; Hare, J. P.; Reeves, C. L.; Cheetham, A. K.; Rühle, M.; Kroto, H. W.; Walton, D. R. M. *Adv. Mater.* 1**999**, *11*, 655.
(17) Terrones, M.; Terrones, H.; Grobert, N.; Hsu, W. K.; Zhu, Y. Q.; Hare, J. P.; Kroto, H. W.; Walton, D. R. M.; Redlich, P.; Rühle, M.; Zhang, J. P.; Cheetham, A. K. *Appl. Phys. Lett.* 1**999**, *75*, 3932.
(18) Han, W. Q.; Redlich, P.; Seeger, T.; Ernst, F.; Rühle, M.; Grobert, N.; Hsu, W. K.; Chang, B. H.; Zhu, Y. Q.; Kroto, H. W.; Walton, D. R. M.; Terrones, M.; Terrones, H. *Appl. Phys. Lett.* **2000**, *77*, 1807.
(19) Nath, M.; Satishkumar, B. C.; Govindaraj, A.; Vinod, C. P.; Rao, C. N. R. *Chem. Phys. Lett.* **2000**, *322*, 333.
(20) Sen, R.; Satishkumar, B. C.; Govindaraj, A.; Harikumar, K. R.; Raina, G.; Zhang, J. P.; Cheetham, A. K.; Rao, C. N. R. *Chem. Phys. Lett.* **1998**, *287*, 671.
(21) Tang, C. C.; Golberg, D.; Bando, Y.; Xu, F. F.; Liu, B. D. *Chem. Commun.* **2003**, *24*, 3050.
(22) Wei, B. Q.; Vajtai, R.; Jung, Y.; Ward, J.; Zhang, R.; Ramanath, G.; Ajayan, P. M. *Nature* **2002**, *416*, 495.
(23) Jung, Y. J.; Wei, B. Q.; Vajtai, R.; Ajayan, P. M.; Homma, Y.; Prabhakaran, K.; Ogino, T. *Nano Lett.* **2003**, *3*, 561.
(24) Wang, X. B.; Liu, Y. Q.; Hu, P. A.; Yu, G.; Xiao, K.; Zhu, D. B. *Adv. Mater.* **2002**, *14*, 1557.
(25) Huang, S. M.; Man, A. H. *J. Phys. Chem. B* **2003**, *107*, 8285.
(26) Huang, S. M. *Chem. Phys. Lett.* **2003**, *374*, 157.
(27) Singh, C.; Shaffer, M. S. R.; Windle, A. H. *Carbon* **2003**, *41*, 359.
(28) Lee, Y. T.; Park, J.; Yu, S. C.; Ryu, H.; Lee, H. J. *J. Phys. Chem. B* **2002**, *106*, 7614.
(29) Charlier, J. C.; Gonze, X.; Michenaud, J. P. *Phys. Rev. B* **1991**, *43*, 4579.
(30) Sandre, E.; Julien, J. P.; Cyrot-Lackmann, F. *J. Phys. Chem. Solids* **1994**, *55*, 1268.
(31) Stephan, O.; Ajayan, P. M.; Colliex, C.; Cyrot-Lackmann, F.; Sandre, E. *Phys. Rev. B* **1996**, *53*, 13824.
(32) Yan, H.; Li, Q. W.; Zhang, J.; Liu, Z. F. *Chem. Phys. Lett.* **2003**, *380*, 347.
(33) Ruhrnschopf, K.; Borgmann, D.; Wedler, G. *Thin Solid Films* **1996**, *280*, 171.
(34) Otani, T.; Hirata, M. *Thin Solid Films* **2003**, *442*, 42.